

## Statistical Fracture Characteristics of an Isotropic Graphite for HTGR Core Components

Taketoshi ARAI, Yutaka NISHIYAMA  
*Japan Atomic Energy Research Institute, Tokaimura, Japan*  
 Takashi KONISHI  
*Toyo Tanso Co., Ltd., Kagawaken, Japan*

### 1 INTRODUCTION

A high temperature gas-cooled reactor (HTGR) is one of the next generation power reactors because of a highly inherent safety and a wide range of industrial applications. The technological potential of HTGRs is attributed to ceramic fuels and graphite core structural components. Graphite materials, however, differ from metallic materials in many respects. Needs to develop the technical bases for the graphite structural design have been evolved in the course of the long HTGR developments. The underlying reasons are :

- (1) Reliable design goals are comparable to those for metallic nuclear components as exemplified in the ASME B & PV Code Sec. III, which features "Design by Analysis".
- (2) Graphite materials possess pseudo-brittleness, suffer irradiation-induced changes and oxidation-induced degradations.
- (3) Graphite core components function as load carrying members with certain design lives.

As a first step in the refinement of graphite structural design codes, the extensive review discussions have been made in the USNRC (Svalbonas et al. 1973). Since then, the subject has been discussed in the international meetings (Bodmann 1986 : Alloway et al. 1986 : Arai et al. 1986 : Prince and Brocklehurst 1986 : Schmidt 1989 : Iyoku et al. 1989). In the meantime, studies on mechanical properties have posed many questions because it has been found almost impossible to propose general design rules from many different observations which are sometimes contradictory among the various kinds of graphites from different manufacturing routes. Therefore, JAERI decided to pursue the practical engineering approach to propose the fracture criteria and the stress analysis methods with limited relevance to the graphite components in the High Temperature Engineering Test Reactor (HTTR) (JAERI 1990). They are classified into the replaceable core components or the permanent core support components. Considering respective service requirements, three grades of graphite and carbon materials were selected by the extensive scoping experiments. A fine-grained isotropic graphite grade IG-110 was specified as a material for the core components. The tests to elucidate and/or verify brittle fracture characteristics of IG-110 graphite and components composed of mechanical testings with normal small specimens and semi-scale component tests on special structural systems. As a result, the structural design guidelines has been proposed (HTTR Design Lab. 1989). The guidelines feature several ingredients which were based on the observations on static uniaxial, multiaxial strengths and low cycle fatigue strengths of the specified graphites.

This paper summarizes the statistical assessments of the uniaxial tensile and compressive strengths, multiaxial fracture stresses and low cycle fatigue strengths of unpurified grade, IG-11 SMIRT 11 Transactions Vol. G (August 1991) Tokyo, Japan, © 1991

The present study is in support of the development of the reliability-oriented (partly reliability design) definitions of the design material strengths.

## 2 EXPERIMENTALS

### 2.1 Material and test specimens

IG-110 graphite is manufactured by Toyo Tanso Co. Ltd.. Typical manufacturing features and mechanical properties of IG-11 graphite are shown in Table 1. In various test programs full-sized logs with some differing dimensions and some different types of test specimens were used, as shown in Table 2. Each program employed 20 or more test specimens at the same loading condition to characterize the statistical variation and the dependence of test specimen orientation (A or L : axial and R or T : radial with respect to the longitude of the original logs. All test specimens were machined from part or whole of the original logs.

Table 1 Some properties of IG-11 graphite

Manufacturer	Toyo Tanso (Japan)	
Filler coke type	Petroleum coke, fine-grained	
Coke grain size (mm)	0.04 (ave.)	
Forming method	Isostatic mold	
Typical log size (m)	∅0.4 x 0.9	
Bulk density (g/cc)	1.78	
Max. HTT (°C)	~3000	
Elastic modulus (GPa)	L	10.1
Tensile strength (MPa)	L	28
Compressive strength (MPa)	L	81

### 2.2 Strength testing methods

The uniaxial tensile and compressive tests (Test A through Test G) utilized the conventional mechanical testing machines with a crosshead speed of 15~80  $\mu$  m/s. The strength tests under biaxial loadings used the two mechanical testing machines specially designed for the same dumbbell type thin-walled tubular test specimens. One applies for tension-compression stress states developed by axial compression or tension together with torsion and the other for tension-tension stress states developed by axial tension with internal pressure. The inner surface of the test specimens for biaxial tension tests were coated with an epoxy adhesive. In both types of biaxial fracture tests the loading rate was fixed to be 0.04 MPa/s in tension.

The dumbbell type specimens were fatigue tested using a servo-hydraulic fatigue testing machine. The loading rate with a triangular wave form was 3.75 kN/s. The stress ratio  $R = -1$  was chosen because the stress cycle would be predominant in the core components (Iyoku et al. 1990). All strength tests above were conducted in air at room temperature. The stress calculation involved in the present study follows the elastic theory.

## 3 RESULTS AND DISCUSSIONS

### 3.1 Uniaxial tensile and compressive strengths

The mean and the coefficient of variation of the individual tests are listed in Table 3. It was found that both tensile and compressive strengths change little among production lots and possess no appreciable anisotropy. In addition, Test F resulted in a good homogeneity of properties within the logs tested (Arai, Sato and Schiffers, 1991). These measurements justify the merge of the individual data to be treated as statistical samples from the same population. Therefore, all tensile strength data (362 points) and compressive strength data (373 points) are plotted in the normal probability scheme in Fig. 1 and Fig. 2, respectively. Obviously both uniaxial strengths are represented as a whole by normal distribution functions. It should be

emphasized that the two-parameter Weibull distribution was not proved justifiable for both uniaxial strengths of IG-11 graphite. There were other evidences on little dependence of tensile strength on effective stress volume (Yoda et al. 1987 : Arai and Konishi et al. 1991). These statistical characteristics led to the unanimous conclusion that the uniaxial strengths of IG-11 graphite should be treated as normal statistical variables. Then, the fact makes it possible to define the specified minimum ultimate tensile (SMUTS) and compressive (SMUCS) strengths as lower tolerance limits for reliability-oriented design and material acceptance procedure which are employed currently in the aerospace industries (Kamiyama 1984). The HTTR design guideline employs the SMUTS and the SMUCS which are determined by the following equation :

$$SMUTS \text{ or } SMUCS = \bar{X} - \left( \alpha + \frac{\beta}{\sqrt{N}} \right) s \quad (1)$$

where  $\bar{X}$  and  $s$  are the mean and the standard deviation of the sample size  $N$ .  $\alpha$  (=2.326) and  $\beta$  (=1.645) are the constants specifying a 99% survival probability with a 95% confidence level according to the standard normal distribution.

### 3.2 Biaxial strengths

Figure 3 shows the normal probability plots of the maximum principal stress at fracture under tension-compression (T-C) stress states. The figure demonstrates that the fracture stress can be approximated by the normal distribution functions whose standard deviation decreases with decreasing maximum principal stress component. All the test results in the fourth quadrant in

Table 2 Summary of strength test programs for IG-11 graphite

	A	B	C	D	E	F	G	H
Reported year	1981	1981	1982	1983	1984	1986	1989	1990
Log size	φ380×720	230×540×850	φ380×700	230×540×850×2 300×540×850×12	φ430×900	φ430×900	150×150×400	300×540×850
Tested block	φ380×420	230×540×150	20×180×700	230×540×100×2 100×540×425×2	φ430×900	φ430×900	150×150×400	300×540×850
Tensile test								
Specimen type and G.L. dimension	Dumbbell φ6×20	Dumbbell φ6×20	Dumbbell φ4.5×9	Dumbbell φ8×30	Dumbbell φ5×21	Dumbbell φ5×21	Dumbbell φ10×20	Dumbbell/Tube φ16×t2×30
No. of specimen A	40	20	53	70	34	64	25	20
R	40	—	—	70	35	65	—	20
Compressive test			(Dumbbell)					
Specimen dimension	φ6×12	φ6×12	φ4.5×9	10×10×10	—	6×6×12	—	—
No. of specimen A	59	40	54	70	—	31	—	20
R	80	—	—	70	—	31	—	—

\*Dimension in mm

Table 3 Summary of individual strength tests on IG-11 graphite

Test		A	B	C	D	E	F	G	H
Tensile strength	A	24.8/7.3	26.5/9.4	25.5/7.1	26.1/7.3	26.1/7.3	25.8/7.0	27.8/5.4	26.3/4.1
MPa	R	24.0/15	—	—	24.4/10	25.7/8.6	25.6/9.4	—	27.3/7.1
Compressive strength	A	73.4/6.0	83.8/5.7	80.9/3.9	79.0/4.8	—	78.5/4.5	—	79.7/3.3
MPa	R	69.6/6.5	—	—	78.9/6.3	—	76.3/3.9	—	—

\*(Mean/Coeff. variation)

the biaxial principal stress domain are depicted in Fig. 4. In the figure is drawn the solid line according to a modified strain energy criterion. The criterion was proposed on the basis of the biaxial fracture tests of a high density graphite (Ely 1968). As shown in Fig. 5, it provides the good agreement with the present observations. The solid line is expressed by the equation below.

$$\left(\frac{\sigma_1}{S_T}\right)^2 - 2\nu\left(\frac{\sigma_1}{S_T}\right)\left(\frac{\sigma_3}{S_C}\right) + \left(\frac{\sigma_3}{S_C}\right)^2 = 1 \quad (2)$$

where  $\sigma_1$  and  $\sigma_3$  are the maximum and minimum principal stresses at fracture, and  $S_T$ ,  $S_C$  and  $\nu$  are the uniaxial tensile strength, compressive strength and Poisson's ratio. It is noted that any other engineering fracture criteria on yielding of metallic materials are not appropriate in predicting observed fracture conditions. Therefore, one can employ the modified maximum strain energy criterion as a basis for defining the design biaxial fracture criterion for the tension-compression stress states of IG-11 graphite. It may be given simply in such a reliability-oriented manner as the uniaxial strengths,  $S_T$  and  $S_C$ , in Eq.(2) are replaced with the SMUTS and the SMUCS as given by Eq.(1), respectively. As a matter of fact, the design criterion is found to be justifiable because as shown in Fig. 5, all measured data lie outside the tolerance limit curve corresponding to a 99% survival probability with a 95% confidence level. Another criterion called a modified Coulomb-Mohr criterion (Paul 1968) may be recommended in favor of simplicity and conservatism (HTTR Design Lab. 1989).

Similar assessments of the fracture characteristics were made on the tests with combined axial tensile load and internal pressure. Fig. 5 reveals the variability of the maximum principal stress at fracture under tension-tension (T-T) stress states. As a result, the statistical variation of the fracture stresses can be represented again well by normal distributions. Fig. 6 shows all measured data for five stress combinations plotted in the axial stress-hoop stress domain. The present data on the equibiaxial tensile stress state gives a significant reduction in fracture stress, i.e. on an average 0.6 times the mean tensile strength ( $S_T$ ). The reduction compares with other noteworthy results of similar experiments: 0.8  $S_T$  for a fine-grained AXF-5Q graphite (Jortner 1972) and 0.6  $S_T$  for a fine-grained 2020 graphite (Ho et al. 1983). On the other hand, as shown in Fig. 6, the fracture conditions under other biaxial tensile stress states are well fitted on an average to the maximum strain energy criterion:

$$\left(\frac{\sigma_1}{S_T}\right)^2 - \left(\frac{\sigma_2}{S_T}\right)^2 = 1 \quad (3)$$

Eq.(3) gives a fracture stress of 0.7  $S_T$  for the equibiaxial tension. Considering these observations on fine-grained graphites, the equibiaxial tensile fractures shall be reexamined further. If Eq.(3) is applicable, a reliability-oriented strength under biaxial tensile stress states is defined similarly as in tension-compression stress states.

### 3.3 Low cycle fatigue strength

Fatigue strength data on IG-11 graphite at  $R=-1$  are shown in Fig. 6. A large variation in fatigue lives were observed at each maximum stress level ( $\sigma_{max}$ ). This specific fatigue behavior may be handled by two engineering methods: statistical method (Price 1978) and probabilistic method (Wilkins et al. 1972). The Price method assumes a statistical treatment of fatigue life ( $N_f$ ) by the following relationship.

$$\log(\sigma_{max}/S_T) = A + B \log N_f + \epsilon \quad (4)$$

where A and B are constants and  $\epsilon$  is a normal distribution function with the mean being zero.

The solid line in Fig. 7 corresponds to the best fitted S-N curve according to Eq.(4). The performance of the Price method is believed to be good when considering no other formula for an S-N curve for metallic materials are of practical use (Brocklehurst 1977 : Ho and Vollman 19 79).

Eq.(4) allows a reliability-oriented design S-N curve to be predicted because the formula given by Eq.(1) involving a normal probability statistics can apply. The lower tolerance limit line corresponds to a 99% survival probability with a 95% confidence level. This statistical approach has been proposed for defining the design constant life fatigue diagrams (Konishi et al. 1989).

The second method called homologous stress method requires the special fatigue test procedures in which the companion test specimens are tensile tested to assess the experimental and theoretical fracture probabilities. The present tests using 25 fatigue test specimens (Test G) provided tensile strengths to be approximated by a normal distribution. The homologous stress  $\sigma_H(i)$  is a probabilistic variable defined by  $\sigma_{max}/S_T(i)$ , where  $S_T(i)$  is an order statistics based on the theoretical distribution of tensile strength with the suffix  $i$  being the  $i$ -th order statistics of the experimental fatigue life  $N_f$ . The method employs the following relationship.

$$\log \sigma_H (i) = C + D \log N_f (i) \quad (5)$$

where C and D are constants. The analyses using Eq.(5) resulted in the solid line in Fig. 8 for the data shown in Fig. 7. It is obvious that the homologous stress method presents a better goodness of fit than the Price method. The interpretation of the observed fatigue fracture characteristics by the homologous stress concept reflects a realistic physical and probabilistic nature of fatigue phenomena of porous polycrystalline graphites. The application to a practical mechanical design, however, has to be coordinated with other current design practices on static strengths mentioned in the preceding sections. Further experiments and analyses are recommended to propose a probabilistic design methodology for brittle structural materials.

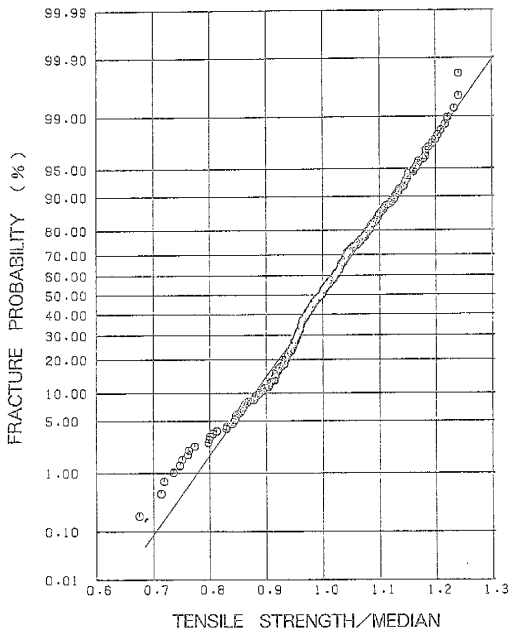


Fig. 1 Normal probability plot of tensile strength data (Median = 25.2MPa)

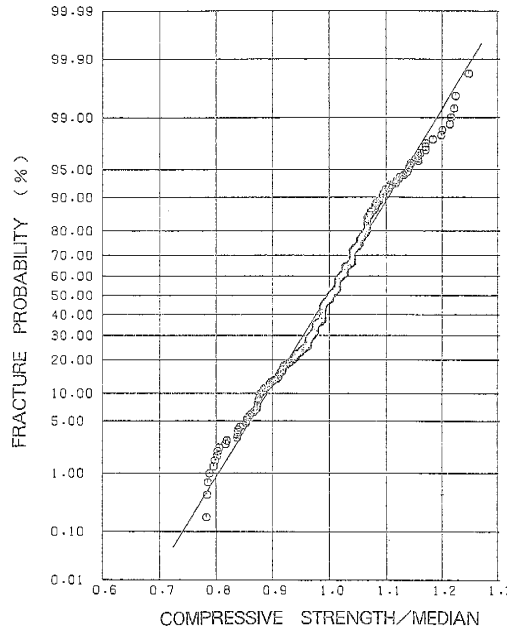


Fig. 2 Normal probability plot of compressive strength data (median = 77.0MPa)

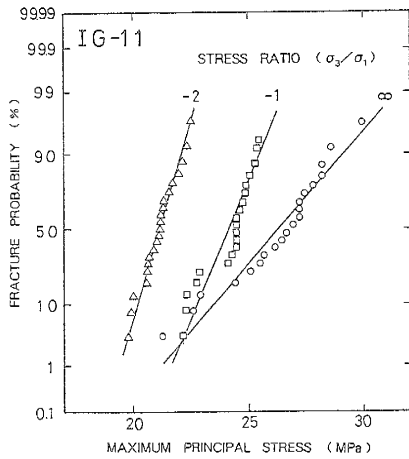


Fig. 3 Normal probability plot of maximum principal stress at fracture under T-C stress states

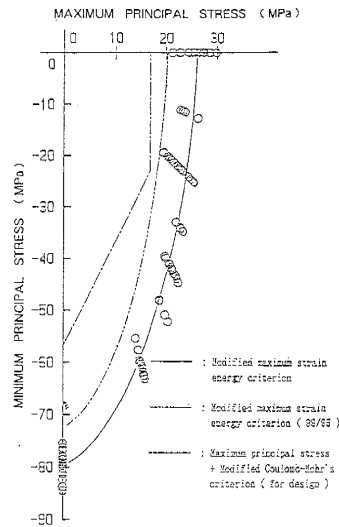


Fig. 4 Fracture stress data and criteria for T-C stress states

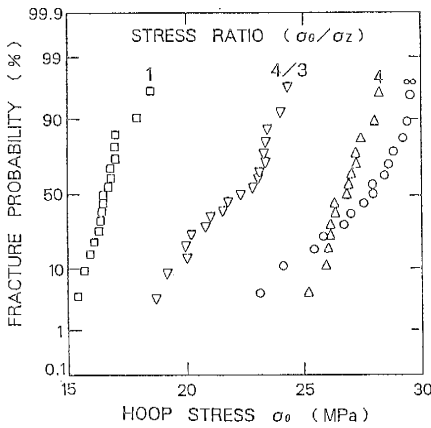


Fig. 5 Normal probability plot of maximum principal stress at fracture under T-T stress states

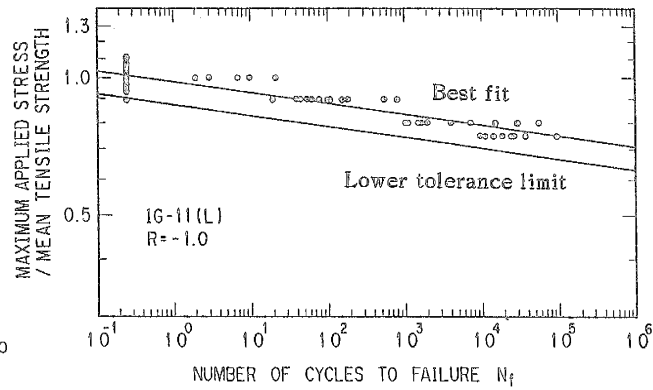


Fig. 7 Fatigue strength data at R = -1 and S-N curve based on Price method

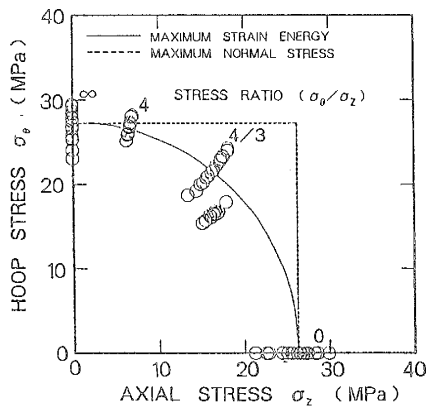


Fig. 6 Fracture stress data and criteria for T-T stress states

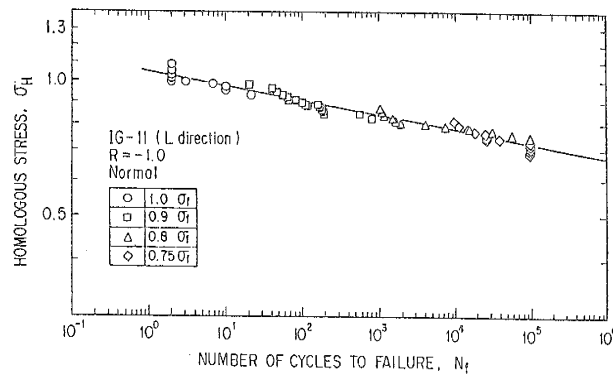


Fig. 8 Fatigue strength data at R = -1 and S-N curve based on homologous stress method